

# LUNG SEGMENTATION IN PULMONARY CT IMAGES USING WAVELET TRANSFORM

Omid Talakoub<sup>1</sup>, Javad Alirezaie<sup>1,2</sup>, Paul Babyn<sup>3</sup>

<sup>1</sup>Department of Electrical and Computer Engineering, Ryerson University, Canada

<sup>2</sup>Department of Systems Design Engineering, University of Waterloo, Canada

<sup>3</sup>Department of Medical Imaging University of Toronto, Canada  
otalakou@ryerson.ca, javad@ryerson.ca, paul.babyn@sickkids.ca

## ABSTRACT

Computer-Aided Diagnosis (CAD) has become a major research interest in diagnostic radiology and medical imaging. The basic goal of CAD is to provide a computer output as a second opinion to assist medical image interpretation by improving accuracy, consistency of diagnosis, and image interpretation time. Since a CAD system is only interested in analyzing a specific organ, segmentation of Computer Tomography (CT) images is a precursor to most image analysis applications. A fully automated method is presented to segment lung in pulmonary CT images based on detected lung edges by wavelet analysis. Due to wavelet transformation characteristics, the proposed method is not only computational inexpensive compared to other existing methods such as snakes or watershed, but also is robust and accurate in detecting lung borders. A set of 330 low dose (50mA) CT images were processed demonstrating accuracy and satisfactory performance of the algorithm.

**Index Terms**— Computer-Aided Diagnosis, Pulmonary CT Images, Wavelet Transformation, Segmentation, Edge Detection

## 1. INTRODUCTION

Computer-Aided Diagnosis (CAD) is a major research interest in diagnostic radiology and medical imaging. Many different types of CAD schemes are being developed for detection and/or characterization of various lesions for variety of imaging modalities, including conventional projection radiography, Computer Tomography (CT), Magnetic Resonance Imaging (MRI) and Ultrasound. Organs currently being targeted by CAD research include breast, chest, colon, brain, liver, kidney, and the vascular and skeletal systems. As segmentation of medical images is often a precursor to image analysis applications, its accuracy is of great concern as segmentation errors may potentially lead to misdiagnosis.

Several methods have been utilized to segment the lung in pulmonary CT images such as thresholding [1], watershed [2], snakes [3], and region growing [4]. Each has its own

drawbacks. Thresholding is the most popular lung segmentation method because it is one of the simplest in methodology and computation. However, it has some drawbacks in lung segmentation. CT lung density is influenced by factors such as subject tissue volume, air volume, image acquisition protocol, physical material properties of the lung parenchyma, and degree of inspiration. These factors make the selection of a single gray-level segmentation threshold difficult, as different thresholds are likely required for different subjects. Although some work has used an adaptive threshold value, this method still has some misregistrations on its segmentation results such as missing boundaries between 2 regions when there is not a significant discontinuity between the boundaries or the borders are too close together. For example, this method requires additional post-processing steps to eliminate the trachea and mainstem bronchi. *Watershed* on the other hand gives an acceptable segmentation result with relatively low computational cost. However, *over-segmentation* is a well-known drawback in watershed segmentation. *Snake* is an active contour which starts from an initial position and shape and fits itself to the shape of a desire object(s). One of the drawbacks of traditional snake model is that the construction of initial contour often requires human interaction and the segmentation results may be heavily sensitive to initial contour conditions. One disadvantage of *region growing* is its computational intensity as well as its performance dependence on its initial seeds.

Edge information in images is an important characteristic of images' content. Conventional edge detection algorithms are typically based on differential operators, such as the Sobel, Prewitt, and Roberts operators. Traditional differential operators work well with edge detection of noiseless images, however in the presence of noise may miss the edges or detect false edges due to the intensity discontinuities. As addressed in [5] and [6], wavelet expansion in higher scales suppress effect of noise on edge detection process. Because of this advantage, several algorithms addressed the edge detection of noisy signal or images, [5, 6, 7, 8, 9]. Medical images are noisy in nature due to limitations of imaging techniques, device noise and health constraints (such as giving minimal ra-

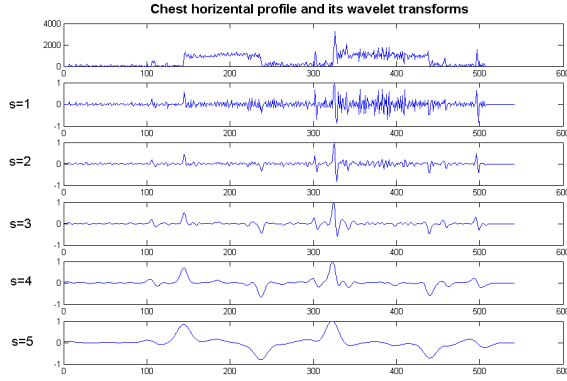


**Fig. 1.** Horizontal profile (shifted by 1000) of lung in a CT image at the top along with its wavelet transformations in dyadic sequence below

diation doses to patients). De-noising as preprocessing step is recommended in CAD systems even though de-noising may suppress some important image edge details; for instance in many techniques edges get blurred as result of de-noising. Therefore algorithms with low sensitivity to noise tend to give higher performance in medical images processing problems.

Wavelet transforms are multiresolution representations of signals and images. They decompose signals into multiscale details by applying a basis function to the signal, [7, 8]. The basis functions used in wavelet transforms are locally supported and they are nonzero only over part of the represented domain. This paper uses wavelet based de-noising because of its ability to eliminate noise due to its subband decomposition algorithm. With the utilized mother wavelet, sharp transitions in images are preserved and depicted extremely well in wavelet expansions. This fact has been examined by several papers on de-noising the MRI images. Xu *et al.* [5] performed wavelet transformation domain filter to de-noise MR head images (SNR 12dB). Karras and Mertzios [10] proposed edge detection in MRI images using combination of wavelet transform and neural network. However to the best of our knowledge, there has been no method proposed to de-noise and segment CT images using wavelet transformation. In order to perform a robust and accurate edge detection, which leads to an accurate segmentation, our proposed algorithm contains the following steps: Image enhancement, 2D Discrete Wavelet Transformation, edge extraction, distinguishing lung border and segmenting the lung region from the entire image.

## 2. METHODOLOGY AND ALGORITHM FOR LUNG SEGMENTATION

Figure 1 shows a horizontal profile taken from a row of an original CT thorax image. The significant discontinuities in this profile occur at the edges, while the small spikes in its

horizontal profile represent image noise and slight changes in body tissues or small objects in the image including small vessels or bronchi. Choosing mother wavelet as derivative of a smoothing function leads to preserving the significant singularities along the scales and vanishing other singularities while we are moving through the scales as described in details at [7, 8, 9] and shown in figure 1. As mentioned earlier, aerated lung pixels have extremely different intensity compared to other surrounding body tissues. In this paper, we considered all the insignificant changes in lung profile as noise since we only interested in distinguishing the lung border, significant discontinuities, in the image. We proposed a wavelet-based method that can overcome these issues and extract actual edges in a pulmonary CT image. Each CT image was enhanced by applying a transformation to its histogram considering that pixel values higher than average body CT value were trimmed to avoid discontinuities detection around bones.

### 2.1. Wavelet Transformation

Points of sharp variation are often among the most important features for analyzing the properties of transient signals or images. They are generally located at the boundaries of important image structures. Singularities are generally characterized by their Lipschitz exponents. The wavelet theory proves that these exponents can be determined from the evolution across scales of the wavelet transform modulus maxima [9]; even smoothness of an edge can be estimated from the decay of the wavelet transform maxima across scales. Lipschitz exponents and smoothing factors are numerical descriptors that allow us to discriminate the intensity profiles of different types of edges [9].

Wavelets are families of functions  $\Psi_{s,t}(x)$  generated from a single base wavelet, called mother wavelet,  $\Psi(x)$  by dilations and translations  $\Psi_{s,t}(x) = 1/\sqrt{|s|}\Psi(\frac{x-t}{s})$  where  $s$  is the dilation (scale) parameter, and  $t$  is the translation parameter. Wavelets must have mean of zero, and the useful ones have localized support in both spatial and Fourier domains. We use the term 2D smoothing function to describe any function  $\theta(x, y)$  whose integral over  $x$  and  $y$  is equal to 1 and converges to 0 at infinity. The image  $f(x, y)$  is smoothed at different scales  $s$  by a convolution with  $\theta(x, y)$ . The direction of the gradient vector,  $\nabla(f * \theta_s)(x, y)$ , at a point  $(x_0, y_0)$  indicates the direction in the image plane  $(x, y)$  along which the directional derivative of  $f(x, y)$  has the largest absolute value. Edges are defined as points  $(x_0, y_0)$  where the modulus of the gradient vector is maximum in the direction towards which the gradient vector points in the image plane. Edge points are inflection points of the surface  $\nabla(f * \theta_s)(x, y)$ . We define two wavelet functions  $\Psi^1(x, y)$  and  $\Psi^2(x, y)$  such that  $\Psi^1(x, y) = \frac{\partial\theta(x,y)}{\partial x}$  and  $\Psi^2(x, y) = \frac{\partial\theta(x,y)}{\partial y}$ . The wavelet transform of  $f(x, y)$  at scale 's' has two components,  $W_s^1 f$  and  $W_s^2 f$ , defined by  $W_s^1 f(x, y) = f * \Psi^1(x, y)$ , ( $i=1,2$ ) Usually, the wavelet model is not required to keep a continuous scale parameter 's'. To allow fast numerical implementations, [9] im-

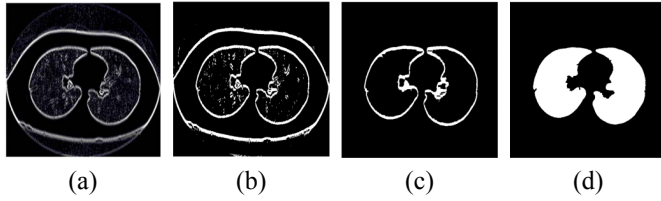


**Fig. 2.** (a) 2D wavelet transformation, shows the high scales (b) edge map image (c) obtained edge mask from high scales. (d) the segmented lung mask.

posed that the scale only varies along the dyadic sequence  $(2^j)_{j \in \mathbb{Z}}$ . Nonorthogonal wavelets are designed to satisfy the required characteristic for detecting lung edges and suppressing noises in the CT images. The mother wavelets are calculated from first and second derivatives of the smoothing function,  $\theta(x)$ , which is basically a low pass filter in Fourier domain. Noise filtration in wavelet domain is based on the fact that sharp edges have large amplitude over the dyadic scales, and noise dies out swiftly while 's' increases. We are using the wavelet transform contents at several adjacent scales to accurately detect the locations of edges and some other fine details. If first derivative of smoothing function is chosen as mother wavelet, the edges will be distinguish as local maxima points. Therefore, by increasing scale only significant maxima, which represent the edge points, will remain over the wavelet transformation and noise will be removed on these scales. In case of choosing the second derivative as mother wavelet, the zero crossing will be considered as location of edges through the scales. However, considering the zero crossing would not give good information on the edge locations since every singularity in the image leads to a zero crossing. So other information should be combined with location of zero crossing in order to distinguish between significant discontinuities and the rest.

The proposed method considers high dyadic scales, above 3, of the wavelet transformation when the first derivative of smoothing function employed in order to determine an approximation of edge locations, the initial edge map. Because those scales do not contain the image's finest details as well as noise, they only represent the significant singularities in the image. By thresholding 2D wavelet transformation of the image on those scales, the initial image's edge map was developed. However, produced edge map represents the edge between lung and other adjunct body parts as well as lung vessels and the other organ body edges such as Thoracic or even surrounding non-body objects. Figure 2(a) and (b) illustrate the wavelet transformation resulted from combination of third and fourth scales and its thresholded image.

## 2.2. Edge map analysis

The next step is to eliminate the objects in the edge map whose area are relatively small in comparison to the size of the image. These objects represent lung vessels or some surrounding non-body objects. Then body outer border was distinguished in the edge map image and eliminated as well as all the edges located outside the body, that are mostly related to CT equipment or objects outside the body. The result is shown in figure 2(c). Upon applying the above mentioned-steps, a mask which is an approximation of lung borders will be obtained. Since thresholded high scales of wavelet transformation

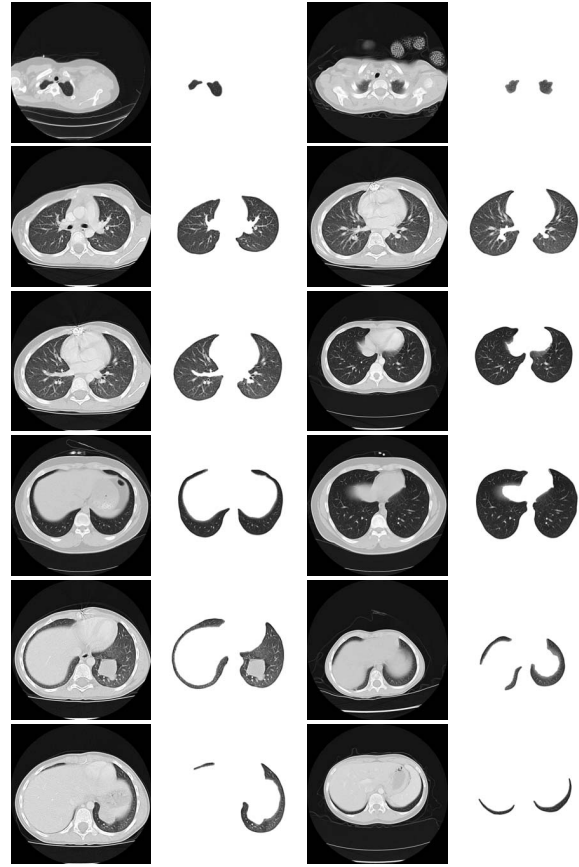


**Fig. 3.** Selected images of several patients along with its corresponding segmentation results

was used, the edge map not only illustrates the edges but also it contains the edge neighbor pixels. The final decision on edge locations was taken based on the first scale information when the second derivative on smoothing function had been used as mother wavelet. The first scale was used since it contains the finest details of edges and its zero crossings accurately represent the lung edges trapped inside the initial mask. This accuracy arises from the significant singularity (contrast difference) between the lung and body voxels. In order to get higher accuracy on reading the zero crossings, the maximas of negative image of wavelet transformation's magnitude along the initial edge map were considered instead of zero crossings. The obtained mask is illustrated in figure 2(d).

## 3. EXPERIMENT

A set of pediatric pulmonary CT images was used to evaluate performance of proposed method in lung segmentation. These images, which are acquired at dose of 50mAs. A database containing 330 DICOM images randomly chosen from randomly selected patients were evaluated by the proposed algorithm. Written software in MATLAB is implemented on a computer with 1.7GHz processing speed with 512MB RAM. The result of this experiment revealed each DICOM image was processed in 2.23Sec on average. Twelve results of this experiment along with the corresponded segmentation results

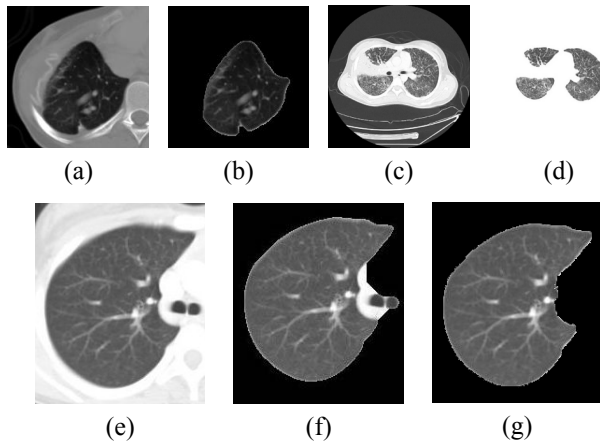


**Fig. 4.** (a) and (b) The dense structures adjunct to the lung border have not been considered as lung area. (c) and (d) Patient with large opacity in his lung. (e) original CT thorax image, (f) segmented lung as result of Dajnowiec algorithm and (g) segmented by the proposed method. Note the more accurate outlining of the lung border along its medial edge.

are listed in figure 3. In order to have visually smooth borders, the lung borders are smoothed by a rolling ball with 3 pixels in diameter.

#### 4. DISCUSSION AND CONCLUSION

We found very close correlation between the actual lung borders and automatically identified borders by computer. The borders were matched except where the lung border had fuzzy edges; even in these cases the difference was less than 3 pixels. Comparison between our segmentation results and manual segmentation of an experienced radiologist proved that the proposed algorithm is capable of segmenting lung in pulmonary CT images with high accuracy. Comparison between obtained results between our proposed method and proposed algorithm by Dajnowiec *et al.* [11], which combines multilevel thresholding with 3D region growing to obtain better performance, on a series of DICOM images proved that our proposed method outperformed the previous algorithm in speed and accuracy. The volume between the manual segmentation and results of each method was considered as segmentation error. The proposed method error was evaluated to be about  $10mm^3$  whereas region growing method error to be in range of  $cm^3$ . An original image and result obtained from each method are illustrated in figures 4 (e), (f), and (g). Additionally, the algorithm should prove its advantage in applications where the processing time is important because of its computational inexpensive nature in compare to other existing segmentation methods. This method does not involve any iterative steps unlike other methods such as Snakes, and Watershed transform where the result has to be modified after each iteration till they meet their termination criteria(s). Secondly, wavelet transformation is not computational expensive. For further reduction in the computation cost, the transformation can be computed with lower computation order upon the numerical implementation of fast wavelet transform algorithms which are given in [9]. In some cases the dense structures adjacent to aerated lung border will not be considered as lung area

as shown in figure 4(a) and (b). This may be an advantage of the proposed method since these profiles contain the wall nodules and should be considered for wall nodule detection purposes. Since the proposed method uses edge information to segment the lung in CT images, the method may have error if the slices get processed independently and a large portion of patient's lung was filled with large opacities in a way that the opacity connects cross borders of lung together as shown in figure 4(c) and (d). However, the 3D rendering of lung or anatomical knowledge can be used to overcome drawback of processing slices independent of each others.

#### 5. REFERENCES

- [1] S. Hu, E. A. Hoffman, and J. M. Reinhardt, "Automatic lung segmentation for accurate quantitation of volumetric x-ray CT images," in *Medical Imaging, IEEE Transactions*, 2001, vol. 20, pp. 490 – 498.
- [2] S. N. Yu and C. T. Chiang, "Similarity searching for chest CT images based on object features and spatial relation maps," in *Engineering in Medicine and Biology Society, EMBC*, 2004, vol. 1, pp. 1298 – 1301.
- [3] Y. Itai, K. Hyoungseop, S. Ishikawa, S. Katsuragawa, K. Nakamura T. Ishida, and A. Yamamoto, "Automatic segmentation of lung areas based on snakes and extraction of abnormal areas," in *Tools with Artificial Intelligence, ICTAI 05. 17th IEEE International Conference*, 2005, pp. 377 – 381.
- [4] C. H. Chuang and W. N. Lie, "Region growing based on extended gradient vector flow field model for multiple objects segmentation," in *Image Processing, International Conference*, 2001, vol. 3, pp. 74 – 77.
- [5] X. Yansun, J. B. Weaver, D. M. Healy, and L. Jian, "Wavelet transform domain filters: A spatially selective noise filtration technique," in *Image Processing, IEEE Transactions*, 1994, vol. 3, pp. 747 – 758.
- [6] Q. H. Lu and X. M. Zhang, "Multiresolution edge detection in noisy images using wavelet transform," in *Machine Learning and Cybernetics*, 2005, vol. 8, pp. 5235 – 5240.
- [7] S. G. Mallat, "A theory for multiresolution signal decomposition: The wavelet representation," in *IEEE Trans. Pa. Anal. Machine Zntell.*, 1989, pp. 674–693.
- [8] S. G. Mallat and S. Zhong, *Complete signal representation with multiscale edges*, New York Univ. Tech. Rep. No. 483, 1989.
- [9] S. Mallat and S. Zhong, "Characterization of signals from multiscale edges," in *Pattern Analysis and Machine Intelligence*, 1992, vol. 14, pp. 710 – 732.
- [10] D. A. Karras and B. G. Mertzios, "On edge detection in mri using the wavelet transform and unsupervised neural networks," in *Video/Image Processing and Multimedia Comm.*, 2003, vol. 4th Conference focused on EURASIP, pp. 461 – 466.
- [11] M. Dajnowiec, J. Alirezaie, and Paul Babyn, "An adaptive rule based automatic lung nodule detection system," in *Pattern Recognition and Image Analysis, Lecture Notes in Computer Science*, 2005, pp. 773–782.